Influence of pyridine versus piperidine ligands on the chemical, DNA binding and cytotoxic properties of light activated *trans*, *trans*, *trans*-$[Pt(N_3)_2(OH)_2(NH_3)(L)]$

Aron F. Westendorf,[a] Lenka Zerzankova,[b] Luca Salassa,[c] Peter J. Sadler[c], Victor Brabec,[b] Patrick J. Bednarski[a*]

[a] Department of Pharmaceutical and Medicinal Chemistry, Institute of Pharmacy, University of Greifswald, Greifswald, Germany

[b] Institute of Biophysics, Academy of Sciences of the Czech Republic, v.v.i., Kralovopolska 135, CZ-61265 Brno, Czech Republic.

[c] Department of Chemistry, University of Warwick, Gibbet Hill Road, Coventry, CV4 7AL, UK.

***** Corresponding author: Tel: ++49 3834 864883; Fax: ++49 3834 864802; email: bednarsk@uni-greifswald.de; address: Institute of Pharmacy, Friedrich-Ludwig-Jahn-Straße 17, 17487 Greifswald, Germany

Part of this work was presented at Eurobic10 from June 22-26, 2010 in Thessaloniki, Greece.

Abstract

The photocytotoxicity and photobiochemical properties of the new complex *trans*, *trans*, *trans*-[$Pt(N_3)_2(OH)_2(NH_3)$(piperidine)] (**5**) are compared with its analogue containing the less basic and less lipophilic ligand pyridine (**4**). The log *P* (n-octanol/water) values were of -1.16 and -1.84 for the piperidine and pyridine complexes, respectively, confirmed that piperidine increases the hydrophobicity of the complex. DFT and TDDFT calculations indicate that **5** has accessible singlet and triplet states which can promote ligand dissociation when populated by both UVA and visible white light. When activated by UVA or white light, both compounds showed similar cytotoxic potencies in various human cancer cell lines although their selectivity was different. The time needed to reach similar antiproliferative activity was noticeably decreased by introducing the piperidine ligand. Neither compound showed cross-resistance in three oxoplatin-resistant cell lines. Furthermore, both compounds showed similar anticlonogenic activity when activated by UVA radiation. Interactions of the light-activated complexes with DNA showed similar kinetics and levels of DNA platination and similar levels of DNA interstrand cross-linking (ca. 5 %). Also the ability to unwind double stranded DNA where comparable for the piperidine analogue (24°, respectively), while the piperidine complex showed higher potency in changing the conformation of DNA, as measured in an ethidium bromide binding assay. These results indicate that the nature of the heterocyclic nitrogen ligand can have subtle influences on both the phototoxicity and photobiochemistry of this class of photochemotherapeutic agents.

Keywords

Platinum azides; cisplatin; photoactivation; cytotoxicity; DNA

1. Introduction

Pt^{IV} diazides have been attracting attention for their potential use as photoactivatable drugs in cancer chemotherapy. [1, 2] Such photoactivatable Pt complexes could increase the therapeutic effect at the site of the tumour while avoiding systemic toxicity typical of traditional Pt anticancer drugs. Towards this end, a number of both *cis*- and *trans*-diazide Pt^{IV} complexes have been synthesized and tested for light-dependent cytotoxicity. Two examples, *cis,trans,cis*-[$Pt(N_3)_2(OH)_2(NH_3)_2$], **1**, and *cis,trans,cis*-[$Pt(N_3)_2(OH)_2$(en)], **2** (**Figure 1A**), have been shown to kill cancer cells in a light-dependent fashion by a mechanism distinctly different from that of cisplatin. [3] Structure activity relationships show that *all-trans* Pt^{IV} diazides are also active; in fact we have found that compounds **3** and **4** are even more potent than their *cis,trans,cis* isomers when activated by light. [3, 4] Furthermore, when ammine or alkyl amine ligands are replaced by pyridine, a 10-fold increase in cytotoxicity is observed when the complexes are irradiated with UVA light. [5] This effect could be related to the decrease in basicity of the coordinating pyridine compared to an ammine or a primary amine ligand. However, introduction of a methyl group at the 2- or 3- position of the pyridine ligand leads to a strong decrease in cytotoxicity while a methyl group in the 4- position has little effect on activity. [5] Thus, steric effects also appear to play a role in the light activation of these photolabile Pt complexes.

To understand better the influence of ligand basicity, lipophilicity and steric effects on the biological activity of this class of *trans,trans,trans*-[$Pt(N_3)_2(OH)_2(NH_3)$(L)] complexes, we have prepared compound **5**, a piperidine analogue of *trans,trans,trans*-[$Pt(N_3)_2(OH)_2(NH_3)$(pyridine)] (**4**). Piperidine is more basic and lipophilic than pyridine but has a comparable steric bulk to pyridine, with a calculated total area of 156 and 127 $Å^2$ and a calculated molecular volume of 135 and 109 $Å^3$ for piperidine and pyridine, respectively. A detailed comparison between the photocytotoxic and photobiochemical properties of

complexes **4** and **5** was therefore made to provide insight into structure-activity relationships in this class of anticancer complexes.

Figure 1

Binding of Pt to DNA is commonly associated with the anticancer activity of cisplatin and related analogues. [6, 7] Thus, in addition studying the cytotoxic effects on cancer cell lines we have also characterized the interactions between DNA and the photoactivated Pt^{IV} diazides in order to investigate similarities and differences in binding that might explain some of the biological effects of these compounds.

2. Materials and methods

Caution! Although no problems were encountered during this work, heavy metal azides are known to be shock-sensitive detonators, therefore it is essential that any platinum azide compound is handled with care.

2.1. Chemicals and cell lines

Cisplatin was from Chempur (Karlsruhe, Germany). Oxoplatin was a gift of the RIEMSER Arzneimittel AG, Germany. Compounds **3** and **4** were synthesized as previously described. [3, 4] Stock solutions of cisplatin and oxoplatin were prepared in DMF (Sigma) and stored at -20 °C. All culture reagents were obtained from Sigma-Aldrich.

To investigate the phototoxic potency of the compounds, six different human cancer cell lines were used: 5637 (bladder), Kyse-70 (esophageal), SISO (cervix adenocarcinoma), DAN-G (pancreatic), A-427 (lung) and HL-60 (acute myeloid leukemia). All cell lines were

obtained from the German Collection of Microorganisms and Cell Cultures (DSMZ, Braunschweig, Germany). A mycoplasma screen was done by using the Hoechst staining method and all cell lines where found to be free of mycoplasms. The oxoplatin resistant cell lines 5637-OXO, SISO-OXO and Kyse-70-OXO were established by weekly exposures to oxoplatin over several months and were resistant to both oxoplatin and cisplatin.

2.2. Light Source

Luzchem Expo panels (Luzchem Reasearch Inc., Ontario, Canada) were used for irradiation. The two Expo panels were accommodated with five fluorescent lamps each, 8 W per lamp. UVB radiation was cut off by a filter. The light source was positioned 25 cm away from the samples giving an intensity of 0.12 mW/cm^2. Cool white fluorescent mercury tubes, 8 W, where used for irradiation with white light (intensity of 0.65 mW/cm^2). The above described set up was used in all cell experiments. All other experiments were irradiated using the LZC-4V illuminator (photoreactor) (Lutzchem, Canada) with temperature controller and UVA tubes (2 mW/cm^2; λ_{max} = 365 nm).

2.3. Preparation of 5

Compound **5** was prepared in a three step synthesis:

2.3.1. *trans*-[$PtCl_2(NH_3)(pip)$]

Piperidine (2.5 mmol, 248 µl) was added to a 4 ml cisplatin (0.200 g, 0.67 mmol) suspension in water. After stirring at 75 °C for 120 min, the colorless solution was cooled to room temperature and reduced to dryness. HCl (2 M, 4 ml) was added to the resulting white solid and stirred at 70 °C for 4 days. The solution was cooled on ice before filtering off the

yellow precipitate, washed with ice cold water, ethanol and diethyl ether and dried under vacuum. Yield: 87% (202.7 mg) of a yellow powder.

2.3.2. *trans,trans*-[$Pt(N_3)_2(NH_3)(pip)$]

Trans-[$PtCl_2(NH_3)(pip)$] (0.4 mmol, 150 mg) was suspended in 50 ml H_2O. After adding $AgNO_3$ (0.8 mmol, 68 mg) the solution was stirred at 60 °C for 24 h in the dark. Forming removal of AgCl on a sintered funnel, NaN_3 (0.8 mmol, 52 mg) was added to the solution. After stirring over-night the volume was reduced to ca. 2 – 4 ml and stored at 4 °C for 24 h. The yellow precipitate was filtered off, washed (ice cold water, ethanol, diethyl ether) and dried under vacuum. Yield: 80% (122 mg) of a light brown powder.

2.3.3. *trans,trans,trans*-[$Pt(N_3)_2(OH)_2(NH_3)(pip)$] (5)

To a solution of *trans,trans*-[$Pt(N_3)_2(NH_3)(pip)$] (0.315 mmol, 120 mg) in 300 ml water, H_2O_2 (30%, 1.9 mmol, 0.195 µl) was added and stirred in the dark overnight. The volume was reduced to ca. 25 ml and filtered off. The volume was then reduced and dry acetone was added to precipitate the final product, which was collected by filtration and washed with ice cold water, ethanol and diethyl ether. Yield: 76 mg (58%) of a bright yellow powder.

IR-Spectra were recorded with a Nicolet IR-200 Ft-IR from Thermo Scientific. The IR-band at 3509 cm^{-1} is assigned to N-H and O-H stretching vibrations. N-H bending vibration is present at 1660 cm^{-1} (m) 1598 cm^{-1}(w) and 1258 cm^{-1} (m). The azide ligand is assigned the band at 2030 cm^{-1}. The C-H stretching vibration gives a band at 2949 cm^{-1} (s), C-H bending at 1448 cm^{-1}, and the band at 1078 cm^{-1} is due to C-N stretching vibrations. A band at 544 cm^{-1} is assigned to a Pt-N vibration.

^{195}Pt NMR spectra for D_2O solutions were recorded on a Bruker 400 NMR (86MHz) and were externally referenced to potassium hexachloroplatinate. A chemical shift of 919 ppm was found for *trans, trans, trans*-[$Pt(N_3)_2(OH)_2(NH_3)$(pip)], which agrees with published ^{195}Pt NMR data for other Pt^{IV} compounds. [8, 9]

The identity and purity of compound **5** was further confirmed by LC/MS (Shimadzu High Perfomance Liquid Chromatograph/Mass Spectrometer). Calculated m/z for $[C_5H_{15}N_8O_2Pt]^-$ ([M-H^-) 414.0971; found 414.0965. HPLC of **5** gave a purity of 97%.

The UV-Vis-spectra (**Figure 1B**), recorded with a Hitachi U-2810 spectrophotometer in H_2O showed a maximum at λ = 287.5 nm with ε = 15,355 $M^{-1}cm^{-1}$. A shoulder was observed at 350 nm and a maximum with a weak intensity was found at ca. 420 nm (ε = 115 $M^{-1}cm^{-1}$).

2.4. Measurement of log *P*

To determine the partition coefficient (*P*) the shake flask method was used. Water and n-octanol were pre-saturated with n-octanol and water, respectively. Compounds were first dissolved in water. Three different ratios of octanol/water were used (e.g. 1:1; 1:2 and 2:1). Mixing was done by vortexing for 30 min at room temperature to establish the partition equilibrium. To separate the phases, centrifugation was done at 3,000 g for 5 min. The platinum concentrations in both phases were determined by flameless atomic absorption spectroscopy (FAAS) with a UNICAM 989 QZ spectrometer.

2.5. Theoretical calculations

All calculations were performed with the Gaussian 03 (G03) program [10] employing the DFT method, the PBE1PBE [11] functionals. The LanL2DZ basis set [12] and effective core potential were used for the Pt atom and the 6-31G**+ basis set [13] was used for all other atoms. Geometry optimizations of **5** in the ground state (S_0) and lowest-lying triplet state (T_1) were performed in the gas phase and the nature of all stationary points was confirmed by normal mode analysis. For the T_1 geometries the UKS method with the unrestricted PBE1PBE functional was employed. The conductor-like polarizable continuum model method (CPCM) [14] with water as solvent was used to calculate the electronic structure and the excited states of **5** in solution. Thirty-two singlet and eight triplet excited states with the corresponding oscillator strengths were determined with a Time-dependent Density Functional Theory (TDDFT) calculation. [15, 16] The computational results are summarized in the Supporting Information.

2.6. Cell growth inhibition with the crystal violet method

Cells were grown in medium containing 90% RPMI 1640 medium and 10% FCS, supplemented with penicillin G (30 mg/l) / streptomycin (40 mg/l) and kept at 37 °C in humidified atmosphere of 5% carbon dioxide/air.

In testing for antiproliferative activity, cells were seeded out in 96-well microtiter plates in 100 µl medium at a density of 1000 cells/well. The plates were returned to the incubator for 24 h. On the day of testing, the stock solutions of cisplatin (20 mM in DMF) were serially diluted two fold in DMF to the desired concentration range, giving a series of five dilutions. Compounds **3**, **4**, and **5** were dissolved in water followed by sterile filtration immediately. Stock solutions and the dilutions were directly diluted 500-fold into medium.

From the working dilutions, 100 µl aliquots were added to each well. When DMF was the solvent, a maximum concentration of 0.1% (v/v) DMF was present.

Compounds **3**, **4**, and **5** were preincubated with the cells for 1 h, followed by irradiation with white light or UVA λ_{max} = 366 nm for up to 30 min. Lower wavelength UV radiation was blocked by a filter for both lamps. Luzchem Expo panels (Luzchem Reasearch Inc., Ontario, Canada) were used for irradiation. The light sources were mounted inside on the roof of the incubator and positioned 25 cm away from the microtiter plates. The plates were incubated for an additional 6 h at 37 °C, then the medium was carefully aspirated off and replaced with 200 µl fresh medium. Ninety hours later the culture medium was discarded and replaced for 25 min with a 1% glutaraldehyde in PBS solution to fix the cells. The fixing buffer was removed and replaced with PBS. Staining was done with a 0.02% solution of crystal violet in water. The dye was added to each well and discarded after 30 min of staining, followed by 15 min washing in fresh water. The cell-bound dye was redissolved in 70% (v/v) ethanol/water and the optical density was measured at λ = 570 nm with an Anthos 2010 plate reader (Anthos, Salzburg, Austria). The IC_{50} values were calculated by a linear least-squares regression of the T/C_{corr} values versus the logarithm of the added compound concentration and extrapolating to the T/C_{corr} values of 50 %. [17] This assay was used for all adherent cell lines.

2.7. Cell growth inhibition with MTT method

The MTT assay was used for determining cytotoxicity in the suspension of cancer cell line HL-60. Cells were seeded out in 96-well microtiter plates in 50µl medium at a density of 10,000 cells/well. Dilutions of the compounds in cell culture medium were added directly to the cultures after seeding. Pretreatment was for 1 h, irradiation with UVA was for 30 min,

followed by a 6 h exposure to the photolyse products. After this time the cells were centrifuged at 500 g for 5 min and the cell pellet was resuspended in fresh medium. The cells were allowed to grow an additional 42 h before the MTT assay was performed. For the MTT assay, 20 µl of a 2.5 mg/ml 3-(4,5-dimethylthiazol-2-yl)-2,5-diphenyltetrazolium bromide (MTT) aqueous solution was added per well and left in contact with the cells in the incubator for 4 h. Prior to measuring the optical density at λ = 570 nm, 100 µl of a 0.04 N hydrochloric acid in 2-propanol solution was added to dissolve the crystalline formazane.

2.8. Determination of oxoplatin cross-resistance

The IC_{50} values of **4** and **5** were determined in three different oxoplatin-resistant human cancer cell lines. The three resistant cell lines were developed in our lab from the wild-type cell lines. The resistance factor (RF) was calculated as follows:

$$RF = \frac{(IC_{50\ -\ \text{oxoplatin resistant}})}{(IC_{50\ -\ \text{wildtype}})} \qquad (2)$$

$IC_{50\text{-oxoplatin resistant}}$ represents the IC_{50} value for the oxoplatin resistant cell line and $IC_{50\text{-wildtype}}$ stands for the IC_{50} value for the wild-type line. The IC_{50} values were determined as described above by the crystal violet assay. Resistance is said to occur when the RF value is greater than 1.5. For comparison, cisplatin and oxoplatin were used.

2.9. Clonogenic Assay

The human cervix adenocarcinoma cell line SISO was used for the *in vitro* clonogenic assay. Cells were seeded in culture flasks and incubated for 24 h. Working solutions of cisplatin (in DMF), **4** and **5** (in water) were diluted 1000-fold into the culture medium at five serial dilutions. After a preincubation time of 1 h, compounds **4**, **5** and control were irradiated for 30 min with UVA λ_{max} = 366 nm. Medium was removed after 6 h and cells were washed twice with PBS before reseeding the cells in six well plates. The culture plates were stored in the dark in an incubator for 10 days. Staining was done with a methylene blue solution (1% in water/methanol 1:1) added for 30 min. After washing out excess dye, the plates were allowed to air dry before manually counting colonies containing 50 or more cells. The plating efficiency (PE) was calculated by:

$$PE = \frac{\text{number of colonies formed}}{\text{number of cells seeded}} \times 100\% \quad (3)$$

The plating efficiency is defined as the ratio of the number of colonies to the number of cells seeded. The surviving fraction (SF), expressed in the terms of PE, is the number of colonies that form after treatment relative to the number of cells seeded.

$$SF = \frac{\text{number of colonies formed after treatment}}{\text{number of cells seeded} \times PE} \quad (4)$$

The IC_{50} values were calculated by a linear least-squares regression of the SF values versus the logarithm of the added compound concentration and extrapolating to the SF values of 50 %. [18]

2.10. Intracellular accumulation of 4 and 5 in the cancer cell line 5637 and comparison to cisplatin

Cells were grown in 25 cm^2 cell culture flasks at 37 °C in a 5% carbon dioxide/air atmosphere to a density of 2 million cells. The cisplatin stock solution was diluted directly into fresh culture medium to a concentration of 50 µM. Solutions of **4** and **5** were freshly prepared in water. After sterile filtration, the stock solutions were directly diluted in fresh culture medium to 50 µM. The flasks were incubated at 37 °C in the dark. After 1 h, the flasks containing **4** and **5** were irradiated for 30 min with UVA λ_{max} = 366 nm. Samples of cisplatin were not irradiated. Controls without irradiation were also performed. After irradiation the flasks were kept in the dark for defined periods of time. For each time point, a flask was removed, the medium was discarded and the cells were washed with ice cold PBS. Cells where trypsinated and suspended in fresh PBS. A 0.5 ml aliquot was used to determine the cell number with a Coulter Counter Z_2 instrument (Beckman-Coulter, Miami, USA). The suspension was centrifuged at 5,000 g for 5 min at -20 °C. The supernatant was discarded and the pellet washed again with ice cold PBS. After a second centrifugation the pellets were frozen at -20 °C until further analysis.

Immediately after thawing the cells were resuspended in a simulated intestinal fluid USP solution and incubated for 15 min at 37 °C to digest the cells. To assure complete destruction of the cells, samples were placed in a sonic bath for another 15 min at 37 °C. Intracellular platinum concentrations were analyzed by flameless atomic absorption

spectroscopy (AAS) as previously described. [19] The results were expressed in terms of ng platinum/1 million cells.

2.11. Polarographic measurement of Pt

Square wave voltammetry was performed with an EG&G Princeton Applied Research Model *384B* Polarographic Analyzer. A three-electrode system was used, comprising an EG&G PARC Model 303A static mercury drop electrode (medium size) and a Ag/AgCl (saturated KC1) reference electrode. All potentials are quoted vs. this reference electrode. Parameters for the square-wave voltammetry operation were as follows: -0.5 V initial potential, -1 V final potential, , 4 mVs^{-1} scan increment, 1 cm^2 electrode area, 50 mV pulse hight, 100 Hz frequency. The electrolyte solution consisted of 1 part 0.08% formaldehyde in 1.5 M H_2SO_4, 1 part 0.008% hydrazine in 1.5 M H_2SO_4, 2 parts water.

Solutions of double-helical calf thymus DNA were incubated with **4**, **5** or cisplatin at the r_i value 0.1 in 10mM $NaClO_4$ at 37 ºC (r_i is defined as the molar ratio of free platinum complex to nucleotides at the onset of incubation with DNA). Immediately after mixing, the solutions containing **4** or **5** were irradiated with UV light for 30 min and then placed in the dark at 37 ºC. Cisplatin- containing solutions were kept in the dark for the whole incubation period. At various time intervals, an aliquot of the reaction mixture was withdrawn and assayed by SW-voltammetry for platinum non-bound to DNA.

2.12. Ethidium bromide fluorescence studies with DNA

In all studies, calf thymus DNA (0.04 mg/ml) was incubated with the platinum complex in 10 mM $NaClO_4$ at 37 °C for 24 h. For cisplatin and [PtCl(dien)]Cl, the incubations were carried out in the dark. For **4** and **5**, samples were irradiated with UVA in the presence of DNA for 30 min and then placed in the dark. After 24 h an ethidium bromide

(EtBr) solution (containing 0.052 mg/ml EtBr and 0.52M NaCl in water) was added to the DNA incubations; the final concentration of EtBr was 0.04 mg/ml, which corresponded to the saturation of all intercalation sites of EtBr in DNA at a concentration of 0.01 mg/ml. After 30 min in the dark at room temperature, fluorescence was measured with a Varian Cary Eclipse fluorescence spectrophotometer, equipped with a 0.5 cm quartz cell, with an excitation wavelength λ = 546 nm and an emission λ =595 nm.

2.13. Unwinding of negatively supercoiled DNA

Unwinding of closed circular supercoiled pUC19 plasmid DNA (2,686 bp) was analyzed by an agarose gel mobility shift assay. [4] The unwinding angle Φ, induced per one molecule bound to DNA was calculated by determining the platinum:base ratio at which the complete transformation of the supercoiled to relaxed form of the plasmid was attained. An aliquot of the sample was subjected to electrophoresis on a 1% native agarose gel running at room temperature in the dark with TAE (Tris–aceate/EDTA) buffer. The voltage was set to 25 V. The gel was stained with EtBr and analysed by photography by using a transilluminator.

The mean unwinding angle was calculated by equation 1:

$$\Phi = -\frac{18\times\sigma}{r_b(c)} \qquad (5)$$

where σ is the superhelical density and $r_b(c)$ is the value of r_b (r_b is defined as the number of molecules of the platinum complex bound per nucleotide residue) at which the supercoiled and nicked forms co-migrate. Higher r_b values above the point of comigratrion cause an increase of migration as positive supercoils are induced.

2.14, DNA Interstrand cross-linking

The levels of interstrand cross-linking by **4**, **5** and cisplatin in linear DNA were measured with pUC19 plasmid (2,686 bp). Linearization was realized by *Eco*RI (*Eco*RI cuts once within the pUC19 plasmid). The linear DNA was 3'-end-labeled by means of Klenow fragment of DNA polymerase I in the presence of [α-^{32}P]dATP and subsequently incubated with platinum complexes. Samples of **4** and **5** were irradiated with the labeled and linearized DNA for 30 min with UVA light immediately after mixing. After irradiation the samples were stored together with cisplatin in the dark at 37 °C. The r_b values ranged for **5** from 0.00003 to 0.002, for **4** from 0.00005 to 0.001 in 0.01 M $NaClO_4$. To each sample of 10 µl, 1µl of 1 mM NaOH and 2 µl of a solution containing 1 mM EDTA, 6.6% sucrose and 0.04% bromophenol blue were added. Samples were analyzed for interstrand cross-links by agarose gel electrophoresis under denaturing conditions (alkaline 1% agarose gel). The intensities of the resulting bands corresponding to single strands, and interstrand cross-linked duplex DNA were quantified by means of a Phosphor Imager (Fuji BAS 2500 system, AIDA software). The Poisson distribution from the fraction of non-cross-linked DNA in combination with the r_b values and the fragment size was used to calculate the percentage of interstrand cross links (the amount of interstrand CLs per one molecule of the platinum complex bound to DNA), see equation 2.

$$\%IEC = -\frac{-\ln ss/100}{r_b \times 5372} \times 100\% \qquad (6)$$

The number of nucleotide residues in the plasmid pUC19 is 5,372. The fraction of DNA molecules corresponding to the non-cross-linked DNA is symbolized with ss, the ration of platinum compound to DNA is given by r_b. [20, 21]

2.15. Statistical analysis

All cell experiments were independently repeated at least three times. The IC_{50} values along with the respective standard deviations were calculated with the software EXCEL (V Microsoft®).

3. Results

3.1. Synthesis of *trans, trans, trans*-[$Pt(N_3)_2(OH)_2(NH_3)(pip)$]

The synthesis of **5** was carried out by a method analogous to that used to synthesize **4**. [3] The new complex was characterized by LC-MS/MS, UV-Vis (**Figure 1B**), IR and ^{195}Pt-NMR. Because heavy metal azido complexes in general can undergo temperature-sensitive detonation, melting point determination and elemental analysis were not preformed. The analytical data are consistent with the structure of **5**.

3.2. Log *P* determinations

The log *P* value plays an important role in ADME studies (**A**bsorption, **D**istribution, **M**etabolism and **E**xcretion) and drug discovery. [22] The traditional shake flask method was used to measure the partition coefficient (*P*) between n-octanol and water.

The log *P* value of -2.21 ± 0.08 we obtained for cisplatin is within the range reported in the literature; i.e., -2.19 and -2.53. [23-26] This value was constant irrespective of whether chloride (100 mM) was present or not. Complexes **4** and **5** are expected to be inert and very stable in water. The log *P* for the *trans* diammine complexe **3** was found to be -2.51 ± 0.14 and is thus even more hydrophilic than cisplatin. For **4** and **5** the log *P* are -1.84 ± 0.06 and -1.16 ± 0.03, respectively. These results are consistent with the order of the log *P* values of the respective amine ligands: pyridine (0.65) < piperidine (0.84) [27, 28], but the relative

difference is greater for the Pt complexes than would be expected from the amine ligands alone.

3.3. Theoretical calculations

Thirty-two singlet excited state transitions were calculated by TDDFT to assign the experimental bands in the UV-Vis spectrum of complex **5**. [29] A good agreement between experimental and theoretical spectra was found, although a small blue shift (ca. 20 nm) is present in the calculated spectrum (**Figure 1B**). The absorption at λ = 278 nm and the shoulder at 350 nm in the experimental data are correctly described by the calculations, as well as the low intensity absorption band at ca. 420 nm. The main band in the UV region is composed by ligand-to-metal charge transfer (LMCT) transitions with N_3^-, OH^- → Pt character. The shoulder has a major inter-ligand (IL) nature, while the lower energy transitions have a mixed LMCT/IL character. All the described transitions have dissociative nature towards the coordinated ligands since they have dominant contributions from the strongly σ*-antibonding LUMO and LUMO+1 orbitals. [30]

Calculation of the lowest-lying triplet geometry can be highly informative [31-33] about the photochemistry of metal complexes. Such a state is generally populated in d^6-metal complexes upon excitation and subsequent intersystem-crossing. [5]

As already observed for other Pt^{IV}-azides derivatives, the lowest-lying geometry of **5** is highly distorted (see supporting information). [30] In fact, the two Pt–N_3 bond distances are elongated by 0.29 Å and 0.42 Å compared to the ground state geometry, possibly indicating that release of azide ligands can occur via triplet formation.

Interestingly, in the triplet geometry the Pt center displays a significantly lower positive charge with respect to the ground state. Such behavior is consistent with the reduction from Pt^{IV} to Pt^{II} observed for Pt^{IV}-azido complexes.

3.4. Influence of light on the cytotoxicity of Pt^{IV}-diazides

The human bladder cancer cell line 5637 was used to study the time-dependent effects of irradiation with UVA of **3**, **4** and **5** on cells. A microtiter assay based on cell staining with crystal violet was used for these studies with adherent cell lines. [34] The MTT assay was used for the suspension cell line HL-60. Cell growth was not influenced by the UV irradiation. In the dark, all three Pt^{IV}-diazide compounds show only weak cytotoxicity. (**Figure 2A**) Irradiation with light of λ_{max} = 366 nm by means of UVA lamps mounted in the ceiling of the cell incubator (UVB light was cut off by a filter) caused an increase of the cytotoxic potential. Complex **3** was less active than **4** and the piperidine analog **5**, while the latter two complexes show comparable cytotoxic potential. (**Figure 2B**) The increased potency of *trans* complexes compared to their *cis* isomers has been reported earlier. [5] In the following experiments **3** was not investigated further due to the comparatively low activity.

Figure 2

To determine the cytotoxic selectivity of **4** and **5**, their IC_{50} values were determined in six different human cancer cell lines.(**Table 1**) The values for **4** range from 30 µM in a human bladder cancer cell line 5637 to 68 µM in a pancreas carcinoma cell line DAN-G. In case of **5**, the IC_{50} values range from 20 µM in the acute myeloid leukemia cell line HL-60 to 80 µM in the esophageal cell carcinoma line Kyse 70. Thus, **5** shows a 4-fold difference in selectivity while **4** only a 2-fold difference between the six cell lines, indicating more selective cytotoxicity of the piperidine complex **5**. Table 1 also shows that compared to cisplatin, the potency of the light-activiated PtIV complexes is 10-20 fold less under identical test conditions (i.e., 30 min irradiation, then 6 h exposure to drug followed by 90 h cell growth

without drug). However, cisplatin showed the same potency in both the light as in the dark, while **4** and **5** are only active when irradiated for 30 min.

Table 1

In studies designed to measure the optimal duration of irradiation, it was found that compound **5** is more rapidly activated than **4**; i.e., only a 10 min irradiation with UVA is required to activate **5** to the same antiproliferative activity as a 30 min irradiation of **4**. (**Figure 3**) This effect was noticeable with both UVA and white light. Thus the introduction of the piperidine ligand leads to a compound that is more efficiently activated by light.

Figure 3

The use of UVA radiation in a therapeutic context is less desirable than longer wavelength light due to the low penetration of UVA into tissue. [35, 36] In order to reach deeper laying tumor tissues, light with longer wavelength is required. Thus, the activation of **4** and **5** was studied with white fluorescent light. **Table 1** shows that the IC_{50} values are up to 2.5-fold higher in some cell lines when irradiated with white light compared to the UVA. Thus, white fluorescence light can also be used to activate both **4** and **5**, and the cytotoxic potency is only marginally decreased.

Treatment with anticancer drugs, e.g. cisplatin and oxoplatin (*cis,trans,cis*-$[Pt(N_3)_2(OH)_2(NH_3)_2]$), often leads to acquired resistance. However, photoactivatable trans-Pt^{IV} diazides might be expected to act by a different mechanism than traditional Pt^{II} complexes. Thus, we investigated whether the new Pt-based drugs can overcome acquired resistance to oxoplatin, a cisplatin Pt^{IV} prodrug, [37] in three oxoplatin resistant cell lines (SISO, KYSE70, 5637). In these cell lines cisplatin is cross resistant to oxoplatin (2- to 3.4-fold resistant). This is consistent with the hypothesis of oxoplatin being a prodrug of cisplatin. On the other hand, **4** and **5** did not show any cross resistance to oxoplatin. (**Table 1**)

3.5. Clonogenic assay in the human cervix adenocarcinoma cancer cell line SISO

The clonogenic assay is an *in vitro* cell survival assay based on the ability of a single cell to grow into a colony and is used to determine cell reproductive death after treatment with cytotoxic agents or ionizing radiation. It represents a more appropriate method than a simple antiproliferative assay to predict antitumor activity. [18, 38] With the SISO human cervix cancer cell line, which grows in well defined colonies, compound **4** is ca. 10-fold more potent in the clonogenic assay compared to the antiproliferation assay (IC_{50} values of 4.94 ± 2.76 and 43.4 ± 23.7 µM, respectively). Compound **5** shows comparable results and is ca. eight fold more potent in the clonogenic than in the antiproliferative assay (values of 5.31 ± 2.84 and 41.8 ± 3.75 µM, respectively). As expected, cisplatin shows potent anticlonogenic activity with an IC_{50} value of 0.20 ± 0.02 µM. Thus, photoactivated compounds **4** and **5** are ca. 25-fold less potent in this assay compared to cisplatin but have antitumor potential and have little toxicity in the dark, in contrast to cisplatin.

3.6. Cellular uptake rates of Pt by 5637 human bladder cancer cells treated with 4, 5 and cisplatin.

Cellular uptake of Pt was studied by FAAS for compounds **4** and **5** in comparison to cisplatin. Cells treated with either Pt^{IV} compound in the dark accumulated only very small amounts of platinum over 8 h while cells exposed to the same concentrations of cisplatin show a continuous uptake of Pt. (**Figure 4**) When the Pt^{IV} compounds are activated by UVA radiation (λ_{max} = 366 nm) for 30 min (indicated by an arrow in **Figure 4**), rapid uptake of Pt takes place. Cells were irradiated for 30 min as in the antiproliferative activity studies. The highest level of Pt (40 ng platinum/1 million cells) is reached after ca. 4 h for **4** and after about 6 h for **5**, respectively. After this time point, a plateau is reached and the cells

accumulate no more platinum. Cells treated with cisplatin show no sign of a plateau after 8 h while accumulating roughly the same levels of Pt compared to the light activated Pt^{IV} compounds.

Figure 4

3.7. Irreversible DNA binding of Pt

Much evidence exists to implicate the binding of cisplatin to DNA as at least one mechanism of anticancer activity. Previous work has shown that **4** can also bind irreversibly to calf thymus DNA when activated by light. [3] Thus, we investigated the effect of the piperidine ligand in comparison to pyridine ligand on the kinetics of binding of UVA activated Pt diazides to calf thymus DNA. Polarography was used to measure the binding of platinum to calf thymus DNA as described elsewhere. [39]

The half-life for cisplatin binding to DNA was found to be 180 min at 37 °C and 24 h; a maximum level of DNA platination of 89% was reached after 24 h (**Figure 5A**). On the other hand, no irreversible binding of either **4** or **5** to DNA was observed when incubations where done in the dark. Interestingly, UVA activated **4** and **5** (i.e., irradiation of complexes for 30 min with light λ = 366 nm) both bind much faster to calf thymus DNA than cisplatin (**Figure 5 B** and **C**); for the UVA-activatable platinum complexes the half-life of binding is less than 5 min. After 25 min a plateau is reached for both complexes, with final levels of platination being very similar for the two compounds; i.e., 86 and 78% for **4** and **5**, respectively.

Figure 5

It has been reported that extracellular concentrations of chloride (e.g. 100 mM) can protect DNA from platination by cisplatin. [40] Likewise, we found that when 100 mM chloride was present in the solutions of DNA, very little platination took place with UVA-activated **4** and **5**. Due to the high chloride concentration, the equilibrium between chlorido and aqua Pt^{II} species is shifted towards the less reactive chlorido species. When cisplatin enters the cell the chloride concentration drops to 4 – 20 mM and the equilibrium shifts to aqua species that bind irreversibly to DNA. Because the same inhibitory effect of chloride was observed with **4** and **5**, it would appear that UVA-activation also leads to the formation of reactive aqua species that can bind irreversibly to DNA.

3.8. Characterization of DNA adducts by ethidium bromide fluorescence.

The fluorescent dye ethidium bromide (EtBr) can be used to distinguish between perturbations induced in DNA by monofunctional and bifunctional adducts of platinum compounds. [41] Binding of EtBr to DNA by intercalation is blocked in a stoichiometric manner by formation of the bifunctional adducts of a series of platinum complexes including cisplatin and transplatin, which results in a loss of fluorescence intensity. [41, 42] On the other hand, modification of DNA by monofunctional platinum complexes such as [PtCl(dien)]Cl (having only one leaving ligand) only results in a slight decrease of EtBr fluorescence intensity as compared with nonplatinated DNA-EtBr complex.

Double-helical DNA was first modified with nonirradiated cisplatin, [PtCl(dien)]Cl and light activated complexes **4** and **5** (for 24 h). The levels of the modification corresponded to the values of r_b in the range between $0 - 0.1$. Modification of DNA by all platinum complexes resulted in a decrease of EtBr fluorescence (**Figure 6**). In accordance with the results published earlier [41-43], monofunctional [PtCl(dien)]Cl only decreased the fluorescence to a small extent. On the other hand, the decrease induced by the DNA adducts of bifunctional cisplatin, and UVA-activated complexes **4** and **5** was considerably more

pronounced. This result suggests that upon irradiation **4** and **5** forms DNA adducts which cannot be grouped, from the viewpoint of their capability to inhibit EtBr fluorescence, with those formed by ”classical” monofunctional platinum(II) complexes. The fact that the decrease of EtBr fluorescence induced by the adducts of UVA activated **4** and **5** was even noticeably more pronounced than that induced by the adducts of cisplatin (**Figure 6**) deserves further discussion. We suggest that the piperidine or pyridine ligand in all or in a significant fraction of adducts of irradiated **4** and **5** (mono- and/or bifunctional) might be well positioned to interact with the duplex. The extent of the observed decrease in EtBr fluorescence indicates that the disturbance of the DNA helical structure by UVA activated **4** and **5** is not only an effect of covalent platinum binding but has to be explained with an additional, perhaps intercalative binding mode. The idea that the piperidine or pyridine ligand in the DNA adducts of UVA activated **4** and **5** interacts with the duplex is further corroborated by the results of DNA unwinding experiments (see the section DNA unwinding).

Figure 6

3.9. DNA unwinding

Electrophoresis in native agarose gel is used to determine the unwinding induced in negatively supercoiled pUC19 plasmid by monitoring the degree of supercoiling. [44] A compound that unwinds the DNA duplex reduces the number of supercoils in closed circular DNA so that their number decreases. This decrease upon binding of unwinding agents causes a decrease in the rate of migration through agarose gel, which makes it possible to observe and quantify the unwinding.

Figure 7 shows electrophoresis gels from experiments in which variable amounts of cisplatin and UVA activated **4** or **5** have been bound to a mixture of relaxed and negatively supercoiled pUC19 DNA. The unwinding angle is given by $\Phi = -18\ \sigma/r_b(c)$, where σ is the superhelical density and $r_b(c)$ is the value of r_b at which the supercoiled and relaxed forms

comigrate.[44] Under the present experimental conditions, σ was calculated to be -0.040 on the basis of data for cisplatin, for which the $r_b(c)$ was determined in this study based on the value σ = 13°. [44, 45] For UVA activated **4** and **5**, $r_b(c)$ was 0.03 (Error! Reference source not found.**B**, **C**, lanes 0.03). The unwinding angle for UVA-activated **4** and **5** calculated in this way was 24 ± 1°, respectively. This unwinding angle is considerably greater than that found for cisplatin. It is reasonable to suggest that the large additional contribution to unwinding is associated with intercalation of the piperidine or pyridine ligands. Thus, the large unwinding angle produced by light activated **4** and **5** is good evidence that the pyridine or piperidine ligand substantially interacts with duplex DNA upon coordiative binding of platinum. In other words, the unwinding angles observed for irradiated **4** and **5** are consistent with DNA binding that involves a combined intercalation/coordination mode similar to that observed for some cationic platinum(II) complexes that carry ethidium [44] or quinoline [46] as a nonleaving group (ethidium and quinoline are well known DNA intercalators which extensively unwind DNA).

Figure 7

The DNA unwinding of the monofunctional, cationic complexes *cis*-$[Pt(NH_3)_2Cl(N3/N8\text{-ethidium})]^+$ was shown to be 19° and 15° for the *N8* and *N3* linkage isomers, respectively. In contrast, the unwinding by *trans*-$[Pt(NH_3)_2Cl(N8\text{-ethidium})]^+$ was only 8°.[44] Complexes containing intercalators, such as *cis*-$[Pt(NH_3)_2Cl(N3/N8\text{-ethidium})]^+$ [44], *cis*-$[Pt(NH_3)_2Cl(N9\text{-9-aminoacridine})]^+$ and *cis*-$[Pt(NH_3)_2Cl(\text{chloroquine})]^{2+}$ [47], form adducts on DNA that produce a situation analogous to monofunctional adducts of irradiated **4** and **5**, i. e., a binding mode compatible with both covalent guanine-*N7* binding and intercalation/stacking of the planar ligand *cis* to the binding site. Coordination of *trans*-$[Pt(NH_3)_2Cl(N8\text{-ethidium})]^+$ to DNA positions the ethidium ligand *trans* to the covalent binding site and directed away from the double helix. In such a binding mode there is very

little contribution from ethidium intercalation to the duplex unwinding. These results and our findings are in accordance with the view that the intercalating moiety needs to be *cis* to the Pt-N7 bond in order to effectively interact with the DNA base stack. The analogy between the above-mentioned cationic *cis*-complexes and irradiated **4** and **5** based on geometric considerations suggests that also monofunctional DNA adducts of the latter compounds may significantly contribute to the unwinding of supercoiled DNA.

3.10. DNA interstrand cross-linking.

The results of previous work indicate that bifunctional platinum compounds form on DNA various types of intrastrand and interstrand cross-links. We also determined in the present work interstrand cross-linking frequency of irradiated **4** and **5** observed for the platination of natural, high-molecular mass DNA. In these experiments pUC19 plasmid (2,686 bp) was used, which was modified by UVA activated **4** or **5** after it had been linearized by *Eco*RI (*Eco*RI cuts only once within pUC19 plasmid). The sample was analyzed for the interstrand cross-links by agarose gel electrophoresis under denaturing conditions. In gel electrophoresis experiments under denaturing conditions, 3'-end labeled strands of linearized pUC19 plasmid containing no interstrand cross-links migrates as a 2,686-base single strand (ss), whereas the interstrand cross-linked strands (ICL) migrate more slowly as a higher molecular mass species. The bands corresponding to more slowly migrating interstrand-cross-linked fragments were clearly noticed if UVA activated **4** or **5** was used to modify DNA fragment at r_b as low as 1×10^{-3} (**Figure 8**). For comparative purposes, the bands corresponding to the modification by cisplatin at $r_b = 0.001$ under identical conditions are also shown (**Figure 8**, lane CDDP). The intensity of the more slowly migrating band increased with the growing level of the modification by **4** or **5** with a concomitant decrease in the intensity of the band corresponding to the non-cross-linked single strand. The radioactivity

associated with the individual bands in each lane was measured to obtain estimates of the fraction of non-cross-linked and cross-linked DNA. The frequency of interstrand cross-links {the amount of interstrand cross-links per one molecule of **4** or **5** bound to DNA} was calculated using the Poisson distribution in combination with the r_b values and the fragment size. [48] The results indicate that light activated **4** and **5** show a similar interstrand cross-linking efficiency (6%) as cisplatin. [20]

Figure 8

4. Discussion

To study the chemical and biological effects of a piperidine versus a pyridine ligand in *trans*-diazido Pt^{IV} complexes, *trans,trans,trans*-[$Pt(N_3)_2(OH)_2(NH_3)$(piperidine)] (**5**) was prepared. The negative octanol/water log *P* values determined for both **4** and **5** show the compounds to be overall hydrophilic, but **5** is noticeably less hydrophilic than **4**. This difference might be expected to affect the biological properties of the compound (e.g., uptake and distribution in cells).

Both compounds have only weak antiproliferative activity in the dark but are selectively activated by either UVA or visible light to potent phototoxins. The UV-Vis spectrum of **5** shows a weak absorption at λ = 420 nm, which corresponds to the HOMO → LUMO and HOMO–1 → LUMO transitions in the calculated electronic spectra. The singlet states accessible through UVA and visible light excitation have all dissociative nature and so has the lowest-lying triplet state. This is related to the contribution of the σ*-antibonding LUMO and LUMO+1 to all transitions. The population of such orbitals is likely to cause ligand dissociation processes.

When activated by either UVA or white light, **4** and **5** show comparable antiproliferative activities across six cancer cell lines, indicating a relatively non-specific mechanism of action. In oxoplatin resistant cell lines, neither **4** nor **5** showed cross-resistance to oxoplatin (a pro-drug for cisplatin). This may be indicative of a different mechanism of

action for the *trans*-diazido complexes compared to cisplatin. So far no *in vivo* antitumor data for these complexes exist, but the positive results of the clonogenic assay indicate that this class of compounds may well have antitumor activity.

Compared to cisplatin, **4** and **5** had a 10-20 fold lower potency to inhibit cell growth when the cells are incubated 6 h with the platinum complexes following light activation. While this is a drastic reduction in activity compared to cisplatin, the clinically used analog of cisplatin, carboplatin, also shows 10-fold greater IC_{50} values compare to cisplatin in our cell lines. [34] However, carboplatin shows reduced side-effects compared to cisplatin, making it a useful therapy for cancer. Thus, not the absolute potency is critical for anticancer activity but rather width of the therapeutic index, and light activated platinum complexes would be expected to have a wider therapeutic index than platinum complexes that are not selectively activated.

One possible advantage of **5** over **4** could be that the former requires less irradiation to reach the same level of antiproliferative activity as the latter. This may be due to the lower hydrophilicity of **5** compared to **4**, which might allow it to cross cell membranes more rapidly. However, Pt uptake studies showed that neither **4** nor **5** are taken up to any appreciable amount by cells in the dark. When both are UVA-activated, the rate of uptake of platinum by 5637 cells is similar for **4** and **5**. This indicates that the photolysis products are selectively taken accumulated by cells while the starting complexes are not. Cisplatin, in contrast, is taken up by cells in the dark to roughly the same levels as light-activated **4** and **5** after 6 h, but shows no signs of plateauing after this time as **4** and **5** did. Likewise, cisplatin showed no difference between antiproliferative potency in the dark or with UVA irraditation.

Like cisplatin both compounds are able to bind irreversibly to DNA after they are photoactivated. This finding suggests that DNA could be one of the targets for the cytotoxic activity, but does not rule out others. UVA irradiation of either **4** or **5** brings about a very rapid platination calf thymus DNA compared to cisplatin; i.e., cisplatin has a half-life of

binding of ca. 180 min, while for **4** and **5** the half-life of binding is less than 5 min. A fast binding mechanism was also described previously for **4** [3], suggesting a novel mechanism of binding Pt to DNA. Nevertheless, the addition of chloride to the DNA solutions prevented binding of Pt to DNA, providing evidence that, like cisplatin, Pt-aqua species are intermediates in the pathway to DNA platination. Moreover, both **4** and **5** showed a similar interstrand-cross-linking efficiency (ca. 5%) compared to cisplatin (ca. 6%), suggesting that the main interactions with DNA are either monofunctional adducts or intrastrand crosslinks. Interstrand crosslinks would be expected to displace ethidium bromide from its intercalation sites in B-DNA and indeed this is observed with both **4** and **5**. The intrastrand crosslinks caused by cisplatin are known to result in the unwinding of super coiled, double stranded DNA, and indeed this was also observed to an even greater extent with both **4** and **5**. Thus, the evidence on interactions with DNA strongly suggests that intrastrand crosslinks are important binding modes for both **4** and **5**.

Nevertheless, the data for three oxoplatin resistant cell lines show no cross-resistance with **4** and **5**, which is inconsistent with the Pt species arising from photolysis acting in a similar way to cisplatin. Alternative mechanisms of cytotoxicity could involve the release of highly reactive azide radicals, which could bring about lipid peroxidation of cell membranes, nitrenes or involve attack on proteins. Further data are needed to verify this idea.

In conclusion, by substituting the pyridine ligand with piperidine a photoactivatable Pt^{IV} diazide was obtained that is less hydrophilic and has a more rapid rate of light activation to cytotoxic species. However, in all other cellular and biochemical aspects (e.g., cellular uptake, kinetics of DNA platination, DNA crosslinks, DNA unwinding, ect.) the behavior of the piperidine complex is similar to that of the pyridine analogue. Thus, the steric bulk of the ligand, not the base strength, appears more important for activity of this new class of photoactivatable anticancer agents.

Acknowledgements

L.S. was supported by a Marie Curie Intra European Fellowship 220281 (PHOTORUACD) within the 7th European Community Framework Programme. We thank the ERC (grant no 247450, BIOINCMED) for support, and members of COST Action D39 for valuable discussions. We also thank the EU for funding bilateral exchanges between Brno (LZ) and Greifswald (AFW).

Figure 1

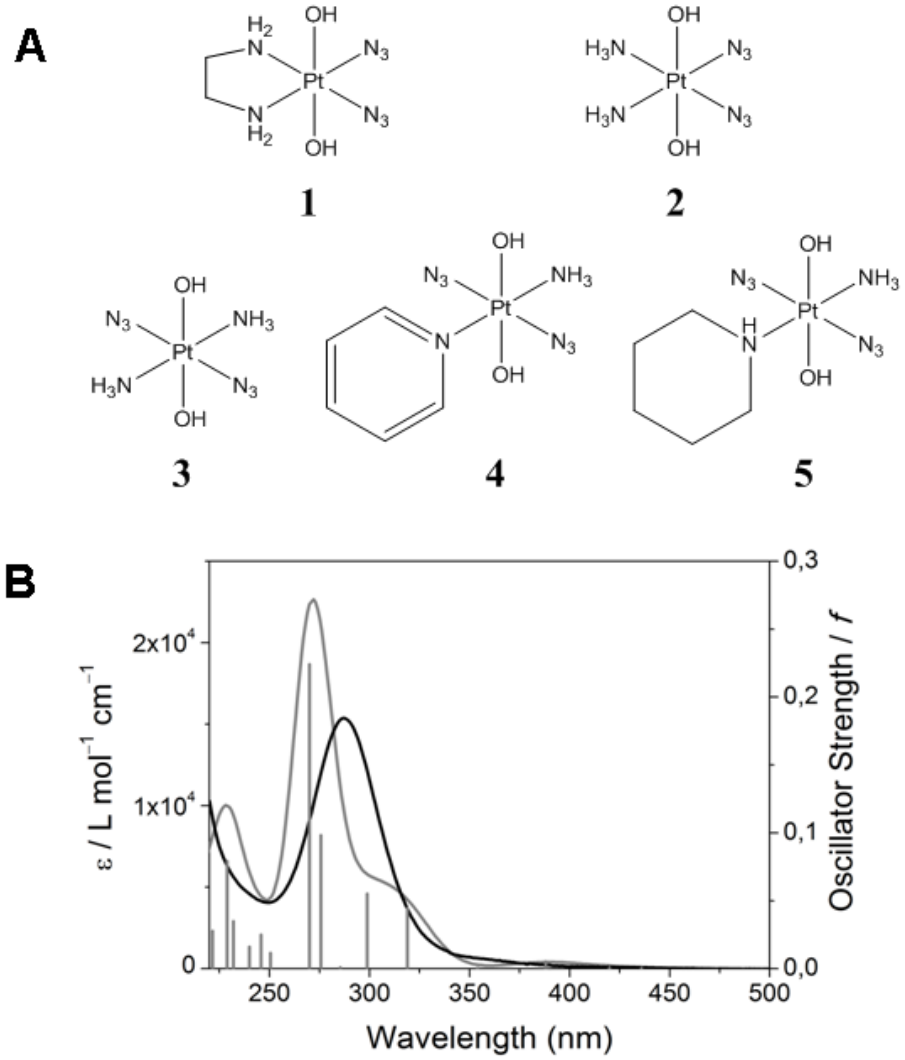
A
1
2
3
4
5
B
ε / L mol⁻¹ cm⁻¹
Oscillator Strength / f
Wavelength (nm)
0
1x10⁴
2x10⁴
250
300
350
400
450
500
0,0
0,1
0,2
0,3

Figure 3

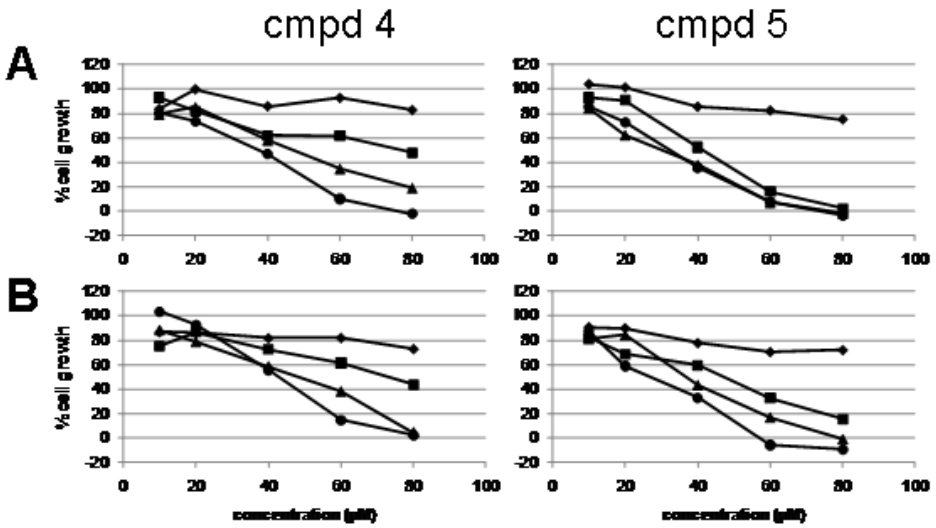

Figure 4

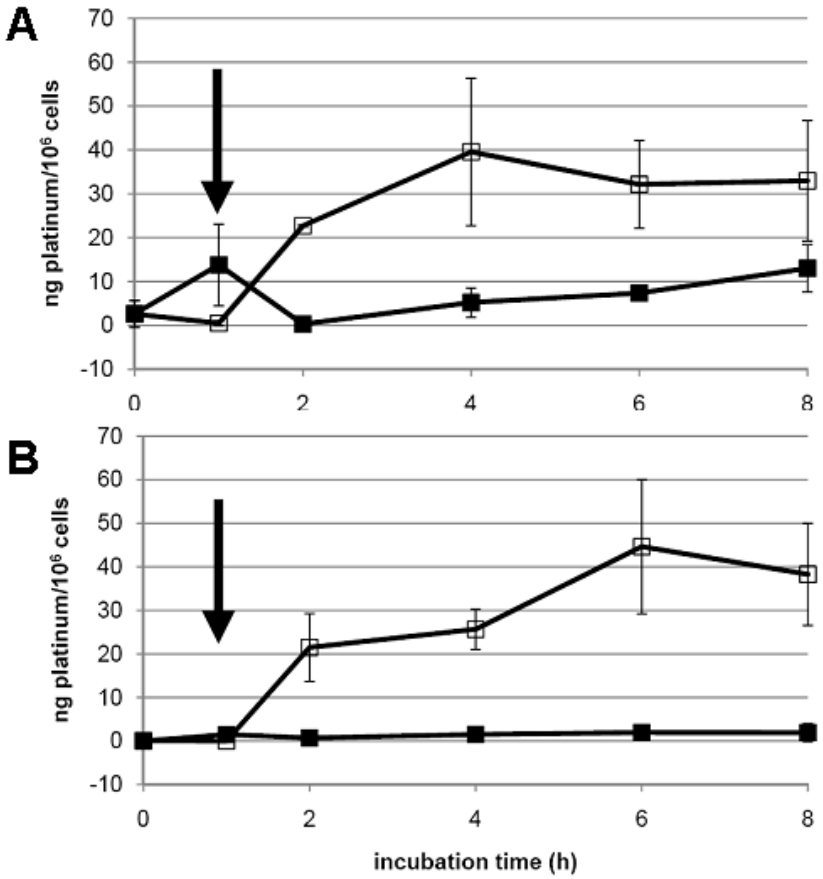
A
B
ng platinum/10^6 cells
70
60
50
40
30
20
10
0
-10
0
2
4
6
8
incubation time (h)

Figure 5

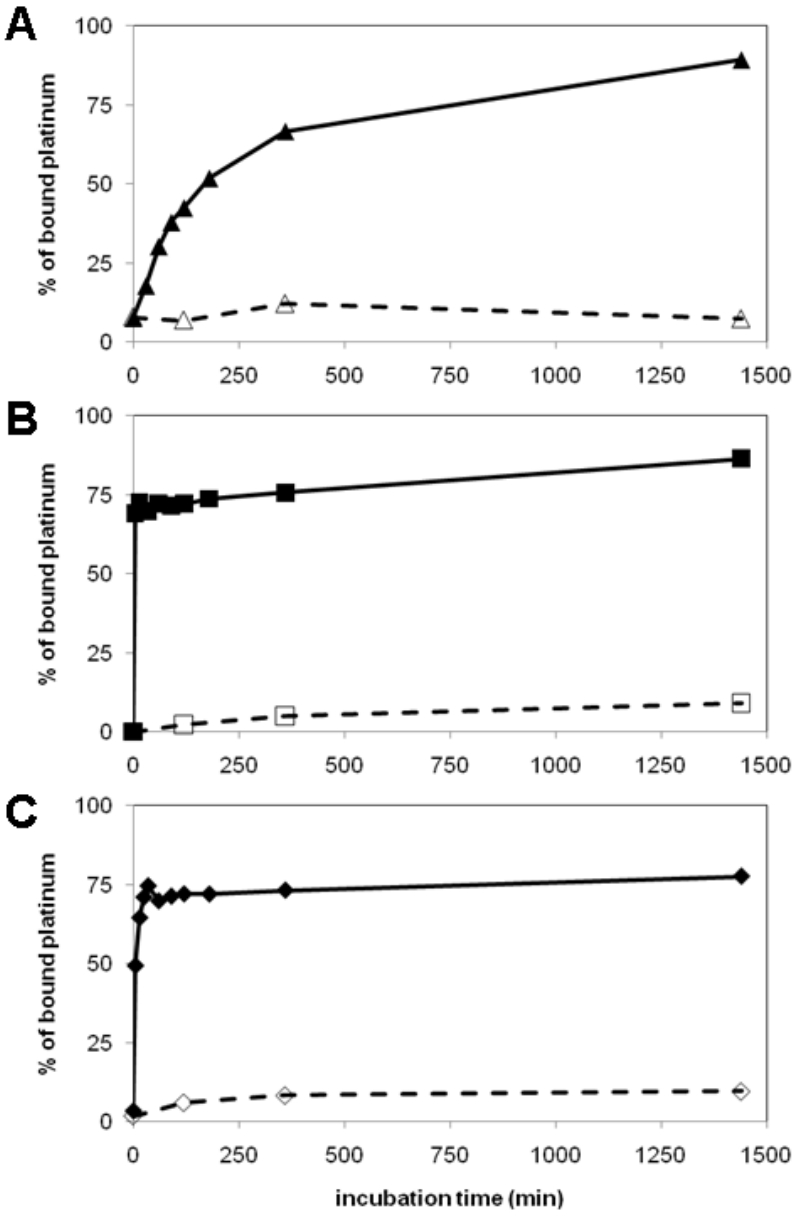
A
B
C
% of bound platinum
100
75
50
25
0
0
250
500
750
1000
1250
1500
incubation time (min)

Figure 6

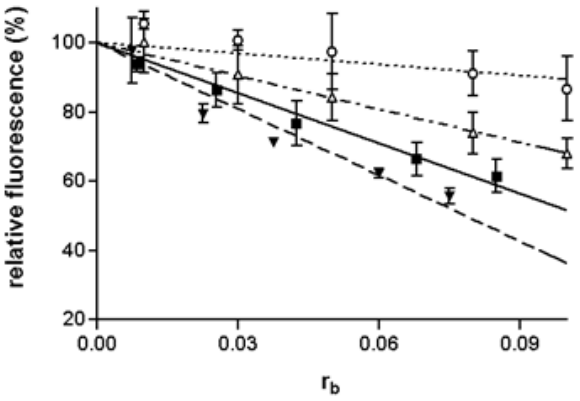

Figure 7

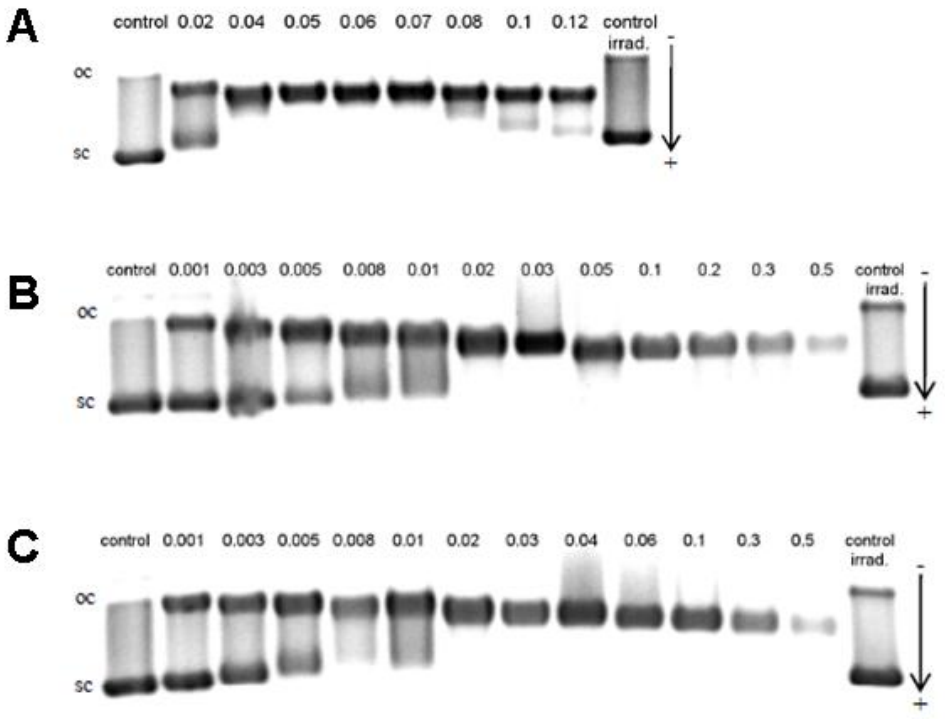
A
control 0.02 0.04 0.05 0.06 0.07 0.08 0.1 0.12 control irrad.
oc
sc
-
+
B
control 0.001 0.003 0.005 0.008 0.01 0.02 0.03 0.05 0.1 0.2 0.3 0.5 control irrad.
oc
sc
-
+
C
control 0.001 0.003 0.005 0.008 0.01 0.02 0.03 0.04 0.06 0.1 0.3 0.5 control irrad.
oc
sc
-
+

Figure 8

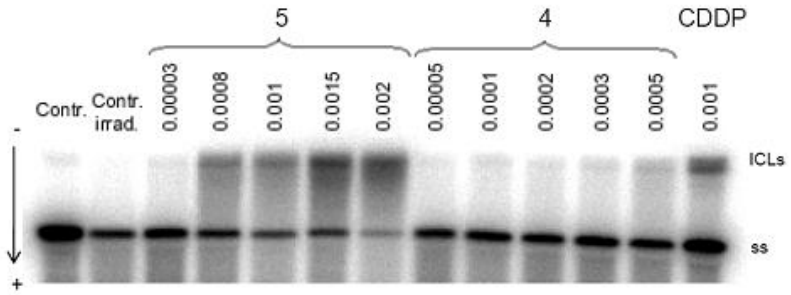
5
4
CDDP
Contr.
Contr. irrad.
0.00003
0.0008
0.001
0.0015
0.002
0.00005
0.0001
0.0002
0.0003
0.0005
0.001
-
+
ICLs
ss

References

[1] P. Müller, B. Schroder, J.A. Parkinson, N.A. Kratochwil, R.A. Coxall, A. Parkin, S. Parsons, P.J. Sadler, Angew. Chem.-Int. Edit. 42 (2003) 335-339.

[2] P.J. Bednarski, F.S. Mackay, P.J. Sadler, Anti-Cancer Agents Med. Chem. 7 (2007) 75-93.

[3] F.S. Mackay, J.A. Woods, P. Heringova, J. Kasparkova, A.M. Pizarro, S.A. Moggach, S. Parsons, V. Brabec, P.J. Sadler, Proc. Natl. Acad. Sci. U. S. A. 104 (2007). 20743-20748.

[4] F.S. Mackay, J.A. Woods, H. Moseley, J. Ferguson, A. Dawson, S. Parsons, P.J. Sadler, Chem.-Eur. J. 12 (2006) 3155-3161.

[5] N.J. Farrer, L. Salassa, P.J. Sadler, Dalton Trans. (2009) 10690-10701.

[6] A.M. Pizarro, P.J. Sadler, Biochimie 91 (2009) 1198-1211.

[7] S.M. Cohen, S.J. Lippard, Progress in Nucleic Acid Research and Molecular Biology, Vol 67, Academic Press Inc, San Diego, 2001.

[8] S.J.S. Kerrison, P.J. Sadler, Dalton Trans. (1982) 2363-2369.

[9] B.M. Still, P.G.A. Kumar, J.R. Aldrich-Wright, W.S. Price, Chem. Soc. Rev. 36 (2007) 665-686.

[10] M.J. Frisch Gaussian 03 revision D 0.1, Gaussian Inc., Wallingford CT, 2004.

[11] J.P. Perdew, K. Burke, M. Ernzerhof, Phys. Rev. Lett. 77 (1996) 3865-3868.

[12] P.J. Hay, W.R. Wadt, J. Chem. Phys. 82 (1985) 270-283.

[13] A.D. McLean, G.S. Chandler, J. Chem. Phys. 72 (1980) 5639-5648.

[14] M. Cossi, N. Rega, G. Scalmani, V. Barone, J. Comput. Chem. 24 (2003) 669-681.

[15] R.E. Stratmann, G.E. Scuseria, M.J. Frisch, J. Chem. Phys. 109 (1998) 8218-8224.

[16] M.E. Casida, C. Jamorski, K.C. Casida, D.R. Salahub, J. Chem. Phys. 108 (1998) 4439-4449.

[17] F. Saczewski, P. Reszka, M. Gdaniec, R. Grunert, P.J. Bednarski, J. Med. Chem. 47 (2004) 3438-3449.

[18] N.A.P. Franken, H.M. Rodermond, J. Stap, J. Haveman, C. van Bree, Nat. Protoc. 1 (2006) 2315-2319.

[19] A.M. Krause-Heuer, R. Grunert, S. Kuhne, M. Buczkowska, N.J. Wheate, D.D. Le Pevelen, L.R. Boag, D.M. Fisher, J. Kasparkova, J. Malina, P.J. Bednarski, V. Brabec, J.R. Aldrich-Wright, J. Med. Chem. 52 (2009) 5474-5484.

[20] V. Brabec, M. Leng, Proc. Natl. Acad. Sci. U. S. A. 90 (1993) 5345-5349.

[21] L. Zerzankova, T. Suchankova, O. Vrana, N.P. Farrell, V. Brabec, J. Kasparkova, Biochem. Pharmacol. 79 (2010) 112-121.

[22] H. van de Waterbeemd, D.A. Smith, K. Beaumont, D.K. Walker, J. Med. Chem. 44 (2001) 1313-1333.

[23] L.I. Feng, A. De Dille, V.J. Jameson, L. Smith, W.S. Dernell, M.C. Manning, Cancer Chemother. Pharmacol. 54 (2004) 441-448.

[24] J.P. Souchard, T.T.B. Ha, S. Cros, N.P. Johnson, J. Med. Chem. 34 (1991) 863-864.

[25] P. Sarmah, R.C. Deka, J. Comput. Aided Mol. Des. 23 (2009) 343-354.

[26] D. Screnci, M.J. McKeage, P. Galettis, T.W. Hambley, B.D. Palmer, B.C. Baguley, Br. J. Cancer 82 (2000) 966-972.

[27] J.W. Li, Chromatographia 60 (2004) 63-71.

[28] H. Sanderson, M. Thomsen, Toxicol. Lett. 187 (2009) 84-93.

[29] F.S. Mackay, N.J. Farrer, L. Salassa, H.C. Tai, R.J. Deeth, S.A. Moggach, P.A. Wood, S. Parsons, P.J. Sadler, Dalton Trans. (2009) 2315-2325.

[30] L. Salassa, H.I.A. Phillips, P.J. Sadler, Phys. Chem. Chem. Phys. 11 (2009) 10311-10316.

[31] L. Salassa, C. Garino, G. Salassa, R. Gobetto, C. Nervi, J. Am. Chem. Soc. 130 (2008) 9590-9597.

[32] L. Salassa, C. Garino, G. Salassa, C. Nervi, R. Gobetto, C. Lamberti, D. Gianolio, R. Bizzarri, P.J. Sadler, Inorg. Chem. 48 (2009) 1469-1481.

[33] S. Betanzos-Lara, L. Salassa, A. Habtemariam, P.J. Sadler, Chem. Commun. (2009) 6622-6624.

[34] K. Bracht, Boubakari, R. Grunert, P.J. Bednarski, Anti-Cancer Drugs 17 (2006) 41-51.

[35] J. Elisseeff, K. Anseth, D. Sims, W. McIntosh, M. Randolph, R. Langer, Proc. Natl. Acad. Sci. U. S. A. 96 (1999) 3104-3107.

[36] V. Barun, A. Ivanov, A. Volotovskaya, V. Ulashchik, J Appl Spectrosc 74 (2007) 430-439.

[37] J. Hamberger, M. Liebeke, M. Kaiser, K. Bracht, U. Olszewski, R. Zeillinger, G. Hamilton, D. Braun, P.J. Bednarski, Anti-Cancer Drugs 20 (2009) 559-572.

[38] T.T. Puck, P.I. Marcus, J. Exp. Med. 103 (1956) 653-666.

[39] Z. Zhao, H. Freiser, Anal. Chem. 58 (1986) 1498-1501.

[40] F.J. Dijt, G.W. Canters, J.H.J. Denhartog, A.T.M. Marcelis, J. Reedijk, J. Am. Chem. Soc. 106 (1984) 3644-3647.

[41] J.L. Butour, J.P. Macquet, Eur. J. Biochem. 78 (1977) 455-463.

[42] J.L. Butour, P. Alvinerie, J.P. Souchard, P. Colson, C. Houssier, N.P. Johnson, Eur. J. Biochem. 202 (1991) 975-980.

[43] V. Brabec, O. Vrana, O. Novakova, V. Kleinwachter, F.P. Intini, M. Coluccia, G. Natile, Nucleic Acids Res. 24 (1996) 336-341.

[44] M.V. Keck, S.J. Lippard, J. Am. Chem. Soc. 114 (1992) 3386-3390.

[45] S.F. Bellon, J.H. Coleman, S.J. Lippard, Biochemistry 30 (1991) 8026-8035.

[46] A. Zakovska, O. Novakova, Z. Balcarova, U. Bierbach, N. Farrell, V. Brabec, Eur. J. Biochem. 254 (1998) 547-557.

[47] W.I. Sundquist, D.P. Bancroft, S.J. Lippard, J. Am. Chem. Soc. 112 (1990) 1590-1596.

[48] N. Farrell, Y. Qu, L. Feng, B. Vanhouten, Biochemistry 29 (1990) 9522-9531.